Since January 2020 Elsevier has created a COVID-19 resource centre with free information in English and Mandarin on the novel coronavirus COVID-19. The COVID-19 resource centre is hosted on Elsevier Connect, the company's public news and information website.

Science of the Total Environment 790 (2021) 148030

Contents lists available at ScienceDirect

Science of the Total Environment

journal homepage: www.elsevier.com/locate/scitotenv

Transformation of antiviral ribavirin during ozone/PMS intensified disinfection amid COVID-19 pandemic

Xiaoyu Liu [a,b,c], Yuntao Hong [a,b,c], Shunke Ding [a,b,c], Wei Jin [a,b,c], Shengkun Dong [d], Rong Xiao [a,b,c], Wenhai Chu [a,b,c,*]

[a] State Key Laboratory of Pollution Control and Resources Reuse, College of Environmental Science and Engineering, Tongji University, Shanghai 200092, China
[b] Ministry of Education Key Laboratory of Yangtze River Water Environment, Tongji University, Shanghai 200092, China
[c] International Joint Research Center for Sustainable Urban Water System, Tongji University, Shanghai 200092, China
[d] School of Civil Engineering, Sun Yat-sen University, Zhuhai 519000, China

HIGHLIGHTS

- PMS/O_3 could efficiently degrade ribavirin, a commonly used antivirals for COVID-19
- Reaction constants of ribavirin with ·OH and $SO_4^{\bullet-}$ were 1.9×10^9 M^{-1} $s^{-1}$and 7.9×10^7 M^{-1} s^{-1}
- The contribution of various reactive species to ribavirin removal by O_3/PMS was evaluated.
- Degradation pathway including dehydrogenation and loss of amide or methanol group was proposed.
- Ozonation and PMS/O_3 system produced much higher brominated OBPs than H_2O_2/O_3 system

GRAPHICAL ABSTRACT

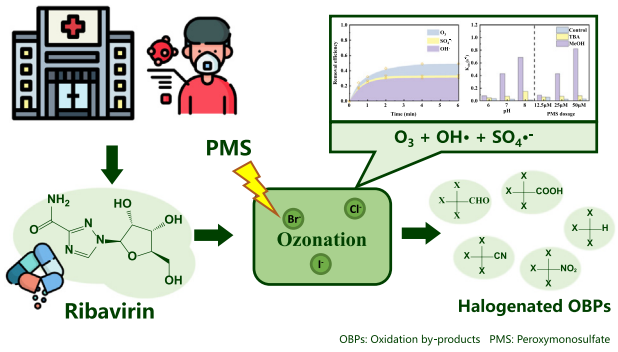

ARTICLE INFO

Article history:
Received 10 March 2021
Received in revised form 18 May 2021
Accepted 22 May 2021
Available online 27 May 2021

Editor: Damia Barcelo

Keywords:
Advanced oxidation process
Ozonation
Peroxymonosulfate
Ribavirin
Oxidation by-products

ABSTRACT

Due to the spread of coronavirus disease 2019 (COVID-19), large amounts of antivirals were consumed and released into wastewater, posing risks to the ecosystem and human health. Ozonation is commonly utilized as pre-oxidation process to enhance the disinfection of hospital wastewater during COVID-19 spread. In this study, the transformation of ribavirin, antiviral for COVID-19, during ozone/PMS-chlorine intensified disinfection process was investigated. •OH followed by O_3 accounted for the dominant ribavirin degradation in most conditions due to higher reaction rate constant between ribavirin and •OH vs. $SO_4^{\bullet-}$ (1.9×10^9 vs. 7.9×10^7 M^{-1} s^{-1}, respectively). During the O_3/PMS process, ribavirin was dehydrogenated at the hydroxyl groups first, then lost the amide or the methanol group. Chloride at low concentrations (e.g., 0.5– 2 mg/L) slightly accelerated ribavirin degradation, while bromide, iodide, bicarbonate, and dissolved organic matter all reduced the degradation efficiency. In the presence of bromide, O_3/PMS process resulted in the formation of organic brominated oxidation by-products (OBPs), the concentration of which increased with increasing bromide dosage. However, the formation of halogenated OBPs was negligible when chloride or iodide existed. Compared to the O_3/H_2O_2 process, the concentration of brominated OBPs was significantly higher after ozonation or the O_3/PMS process. This study suggests that the potential risks of the organic brominated OBPs should be taken into consideration when ozonation and ozone-based processes are used to enhance disinfection in the presence of bromide amid COVID-19 pandemic.

* Corresponding author at: Room 407, National Engineering Research Center for Urban Pollution Control, 1239 Siping Road, Yangpu District, Shanghai 200092, China.
E-mail address: 1world1water@tongji.edu.cn (W. Chu).

https://doi.org/10.1016/j.scitotenv.2021.148030
0048-9697/

1. Introduction

Since the first report of patients with coronavirus disease 2019 (COVID-19) in December 2019, COVID-19 has raised international concern due to its rapid spread, and the pandemic is difficult to control in many countries and regions (Lu et al., 2020a). In order to control the spread of COVID-19, large amount of antivirals such as ribavirin, chloroquine phosphate, alpha interferon, lopinavir and ritonavir have been consumed (Hung et al., 2020; Wong et al., 2021). Ribavirin can be effective against both RNA and DNA viruses, and owing to its broad-spectrum action, it was extensively used to treat viral diseases such as herpes, hepatitis C, and Lassa fever (Ye et al., 2020).

As wastewater treatment processes were not designed for micropollutant removal, up to 20 ng/L of ribavirin was detected in the influent and effluent of wastewater treatment plant previously (Gani et al., 2021; Peng et al., 2014). Despite being low in concentration, potential risks of these antiviral drugs to both human and ecological health are still a concern due to chronic exposure (Nannou et al., 2020). An in vitro bioassay employing human-induced pluripotent stem cells showed that ribavirin could cause DNA damage and the accumulation of reactive oxygen species (Ye et al., 2020). Besides, antiviral resistance may be developed after chronic exposure to antiviral drugs (Nannou et al., 2019). The expanded use of ribavirin during the COVID-19 pandemic probably resulted in the substantial increase of ribavirin in wastewater effluent, especially in hospital wastewater. Therefore, the potentially increased release and transmission of ribavirin from wastewater during COVID-19 pandemic demands attention.

To prevent the transmission of the COVID-19, intensified disinfection has been implemented in hospital wastewater amid COVID-19 pandemic (Chu et al., 2021). Chlorine and chlorine-based disinfectants are commonly-used for disinfection. However, increased chlorine consumption would significantly promote disinfection by-product (DBP) formation, and both residual chlorine and DBPs in wastewater would pose potential risks to aquatic organisms (Liu et al., 2020; Luan et al., 2020). Ozonation is a good candidate due to high disinfection efficiency and limited DBP formation. Previous researches have observed the toxicity of water after ozonation was much lower than that after other disinfection process, and pre-ozonation could decrease chlorine demand in subsequent disinfection, which is especially suitable for hospital wastewater treatment (Han and Zhang, 2018). Besides, micropollutants, undesirable odor and color can be simultaneously removed during ozonation. Therefore, ozonation can be used as an efficient and versatile pre-oxidation process before chlorination. To further increase the oxidation ability of ozonation, several ozone-based advanced oxidation process (AOP) such as O_3/H_2O_2 and O_3/PMS were proposed (Cong et al., 2015; Malik et al., 2020). Addition of peroxymonosulfate (PMS) during ozonation could simultaneously produce hydroxyl radical (•OH) and sulfate radical (SO_4•$^-$) (Malik et al., 2020; Yang et al., 2015). Both •OH and SO_4•$^-$ are non-selective oxidants with high redox potential (1.9–2.7 V for •OH and 2.5–3.1 V for SO_4•$^-$), which can readily react with most organic compounds (Lee et al., 2020; Malik et al., 2020). Considering the high stability and solubility of PMS, adding PMS can be an effective and convenient way to enhance ozonation during COVID-19 spread.

Due to the limited efficiency of conventional wastewater treatment processes on micropollutant removal, residual ribavirin may be transformed alongside other dissolved organic matter (DOM) during disinfection processes (Postigo and Richardson, 2014). Mineralization of micropollutant can only be achieved at high oxidants dosage, and the formed by-products may process higher toxicity than the parent compounds in some cases (Lu et al., 2020b; Peng et al., 2021; Wu et al., 2020). Nowadays, limited work has been done on the transformation of ribavirin during oxidation/disinfection process. To insure the biological safety, more research is needed to reveal the latent risk of O_3/PMS-chlorine intensified disinfection, and the formation of by-products with high toxicity during O_3/PMS-chlorine process should be systemically studied.

This research aims to investigate: 1) the degradation kinetic of ribavirin by O_3/PMS process and the contribution of different oxidants under various reaction conditions; 2) the effect of water matrix (inorganic anions and organic matter) on the degradation efficiency of ribavirin by O_3/PMS process; 3) transformation pathway of ribavirin and formation of halogenated OBPs during ozonation and ozone-based AOPs (O_3/PMS vs. O_3/H_2O_2), and 4) the formation of DBPs during subsequent chlorination.

2. Materials and methods

2.1. Chemicals

Ribavirin, PMS, sodium persulfate (PS), tert-butyl alcohol (TBA), methanol (MeOH), sodium bromide, sodium chloride, potassium iodide, humic acid and sodium hypochlorite were purchased from Aladdin Industrial Inc. (Shanghai, China). All other chemical reagents were of at least analytical grade and obtained from Sinopharm Chemical Reagent Co., Ltd. (Shanghai, China) unless otherwise specified. O_3 stock solution (20–30 mg/L) was prepared by sparging O_3/O_2 gas through 4 °C ultrapure water and the concentration of dissolved O_3 was determined by measuring absorbance at 260 nm ($\varepsilon = 3200\ M^{-1}\ cm^{-1}$) (Mao et al., 2020; Yang et al., 2015). All solutions were prepared using ultrapure water produced from the Milli-Q water purification system (Millipore, USA).

2.2. Experimental setup and design

Batch experiments were carried out in 250 mL conical flask containing 10 μM ribavirin solution under ambient temperature (25 °C), and the pH of solution was buffered with 5 mM phosphate. Reaction initiated once certain volumes of O_3 and PMS stock solution were added. At predetermined time intervals, solution was withdrawn and quenched with excess sodium hyposulfite for further analysis.

To determine the contribution of •OH, SO_4•$^-$ and O_3 to the degradation of ribavirin, second-order rate constants of ribavirin with •OH ($k_{•OH/RBV}$), SO_4•$^-$ ($kso_{4^{-}\cdot/RBV}$) and O_3 ($K_{O3\cdot/RBV}$) were determined in UV/H_2O_2, UV/PS and ozone system, respectively, by competitive dynamics reaction. Benzoic acid (BA) and atrazine (ATZ) with known reaction rate constant with •OH, SO_4•$^-$ and ozone were used as probe compound ($k_{•OH/BA} = 3.90 \times 10^9\ M^{-1}\ S^{-1}$, $kso_{4^{-}\cdot/BA} = 1.2 \times 10^9\ M^{-1}\ S^{-1}$ and $k_{O3/ATZ} = 16\ M^{-1}\ S^{-1}$) (Mao et al., 2020; Tan et al., 2020). Since direct photolysis of ribavirin and BA under the same condition was negligible, the $k_{•OH/RBV}$ and $kso_{4^{-}\cdot/RBV}$ can be calculated as follows:

$$\frac{k_{\bullet OH/BA}}{k_{\bullet OH/RBV}} = \frac{\ln \frac{[BA]_T}{[BA]_0}}{\ln \frac{[RBV]_T}{[RBV]_0}} \quad (1)$$

$$\frac{k_{SO_4^{\bullet -}/BA}}{k_{SO_4^{\bullet -}/RBV}} = \frac{\ln \frac{[BA]_T}{[BA]_0}}{\ln \frac{[RBV]_T}{[RBV]_0}} \quad (2)$$

The steady-state concentration of •OH and SO_4•$^-$ in the process was evaluated by monitoring the degradation of probe compounds (BA and nitrobenzene (NB)) with known reaction constants. Due to different reaction kinetics between probe compounds and oxidants ($k_{•OH/NB} = 5.90 \times 10^9\ M^{-1}\ S^{-1}$, and $k_{•OH/NB} < 10^6\ M^{-1}\ S^{-1}$), steady-state concentration and contribution of •OH and SO_4•$^-$ may be determined by experiment process and kinetic calculation provided in Text S1.

The formation of halogenated OBPs during O_3/PMS, O_3/H_2O_2 and O_3 process in the presence of halide was also investigated, and the experimental procedure was showed in Fig. 1. After 30 min pre-oxidation, 10 mL sample was withdrawn to determine the formation of halogenated OBPs. Besides, another 40 mL sample was put into 40.0 mL brown glass bottles and added appropriate amount of chlorine (4 mg/L or

8 mg/L). After 24 h chlorination at room temperature in the dark, the sample was quenched for further DBP analysis. The ascorbic acid which hardly resulted in DBP hydrolysis and affected DBP detection was chosen as quenching agent. The oxidants were nearly complete consumed after 30 min reaction, which showed limited effect on subsequent chlorination experiments (Table S1).

2.3. Analysis methods

Ribavirin, NB, BA and ATZ were determined by high performance liquid chromatography (HPLC-2010, SHIMAZU, Kyoto, Japan) with a UV detector and an Agilent Shim-pack C18 column (250 mm × 4.6 mm, 5 μm). The detailed parameters of HPLC-UV have been listed in Table S2. OBPs and DBPs including trihalomethanes (THMs), haloacetonitriles (HANs), halonitromethane (HNMs) and haloacetaldehyde (HALs) were quantified by gas chromatography with an electron capture detector (GC-ECD, Shimadzu QP2010plus, Kyoto, Japan) and a RTX-5 column (30 m, 0.25 mm ID, 0.25 μm film thickness, Restek Corporation, Bellefonte, USA). HAAs were derivatised to their corresponding esters using 10% sulfuric acid in methanol (*v*/v), and then measured with a gas chromatography/mass spectrometer (GC–MS-QP2020, Shimadzu Corporation, Japan). The detailed step of OBPs/DBPs analysis was available in previous researches (Fang et al., 2019; Hou et al., 2018) and the limits of detection and quantitation for OBPs/DBPs were available in Table S3. Chlorine concentrations were measured using a portable colorimeter (HACH Pocket Colorimeter TMII, Loveland, CO, USA) and a DPD free chlorine reagent (HACH, Loveland, CO, USA). Dissolved ozonation were determined by indigo regent (HACH, Loveland, CO, USA) and spectrophotometer (HACH DR6000, Loveland, CO, USA). PMS and H_2O_2 concentrations were measured using the ABTS method and potassium titanium (IV) oxalate method (Sellers, 1980; Yang et al., 2015). Dissolved organic carbon (DOC) was measured with a total organic carbon analyser (Shimadzu TOC-VCPH, Kyoto, Japan). The proposed degradation pathways were proposed using TSQ Quantum quadrupole mass spectrometer (ESI-tqMS, Thermo Scientific MAX) with an electrospray ionization (ESI) source, and the detailed experiment steps and parameters were available in Text S2.

The quantum chemical calculation of ribavirin was carried out by Gaussian 09 (Revision C.01) with the input structures created by GaussView 5.0 based on density functional theory (DFT/B3LYP/6-31G (d, p)) (M. J. Frisch et al., 2016).

3. Results and discussion

3.1. Degradation of ribavirin by PMS, O_3, and O_3/PMS

The degradation of ribavirin by PMS alone, O_3 alone, O_3/PMS and O_3/H_2O_2 process was compared in Fig. 2. Less than 5% ribavirin was degraded by PMS alone, which indicated poor oxidation of ribavirin by PMS. The pseudo-first-order rate constants of ribavirin degradation by O_3 and O_3/PMS process were 3.84×10^{-2} and 4.32×10^{-1} s^{-1}, respectively, indicating that PMS could significantly promote the degradation efficiency of ribavirin during ozonation. Similar results were reported in previous research (Cong et al., 2015; Mao et al., 2020). The higher removal efficiencies of the O_3/PMS process were attributed to the increased formation of free radicals (e.g., •OH and $SO_4^{\bullet-}$) from reactions between O_3 and PMS (Eqs. (3)–(6)), and accelerated ozone consumption (Fig. S1) (Yang et al., 2015).

$$SO_5^- + O_3 \rightarrow SO_8^- \tag{3}$$

$$SO_8^- \rightarrow SO_5^{\bullet-} + O_3^{\bullet-} \tag{4}$$

$$SO_5^{\bullet-} + O_3 \rightarrow SO_4^{\bullet-} + 2O_2 \tag{5}$$

$$O_3^{\bullet-} + H_2O \leftrightarrow \bullet OH + OH^- + O_2 \tag{6}$$

As shown in Fig. S2, although ribavirin was effectively eliminated by O_3 and the O_3/PMS process, the decrease of DOC value was negligible, indicating that limited mineralization happened and some intermediates have been produced.

3.2. Contribution of reactive species during O_3/PMS

Previous studies reported that O_3, $SO_4^{\bullet-}$ and •OH made great contribution to the degradation of micropollutant during the O_3/PMS process, which can be described by Eqs. (7)–(8) (Mao et al., 2020; Tan et al., 2020), where [C] and [O_3] represent the concentration of ribavirin and O_3 at specific time, respectively; $[SO_4^{\bullet-}]_{ss}$ and $[\bullet OH]_{ss}$ are the steady-state concentration of $SO_4^{\bullet-}$ and •OH. k' is the pseudo first-order rate constant of ribavirin with specific oxidants, and k represents the apparent second-order rate constants of the reaction between ribavirin and corresponding oxidants.

$$\frac{d[C]}{dt} = k'_{\bullet OH}[C] + k'_{SO_4^{\bullet-}}[C] + k'_{O_3}[C] \tag{7}$$

$$\ln\frac{[C]_t}{[C]_0} = \int_0^t k'_{\bullet OH}dt + \int_0^t k'_{SO_4^{\bullet-}}dt + \int_0^t k'_{O_3}dt = \int_0^t [\bullet OH]_{ss}k_{OH,C}dt + \int_0^t [SO_4^{\bullet-}]_{ss}k_{SO_4^{\bullet-},C}dt + \int_0^t [C]k_{O_3,C}dt \tag{8}$$

Due to negligible degradation of ribavirin by PMS alone (Fig. 3), the contribution of PMS was not considered. According to the result of competitive kinetics experiments (Fig. S2), the second-order rate constants of ribavirin with •OH, $SO_4^{\bullet-}$ and ozone were determined to be 1.9×10^9, 7.9×10^7 M^{-1} s^{-1} and 9.8 M^{-1} s^{-1}, respectively. Therefore, the contribution of different species in the O_3/PMS process could be calculated by the model in Text S1. The result was illustrated in Fig. 3. •OH, $SO_4^{\bullet-}$, and

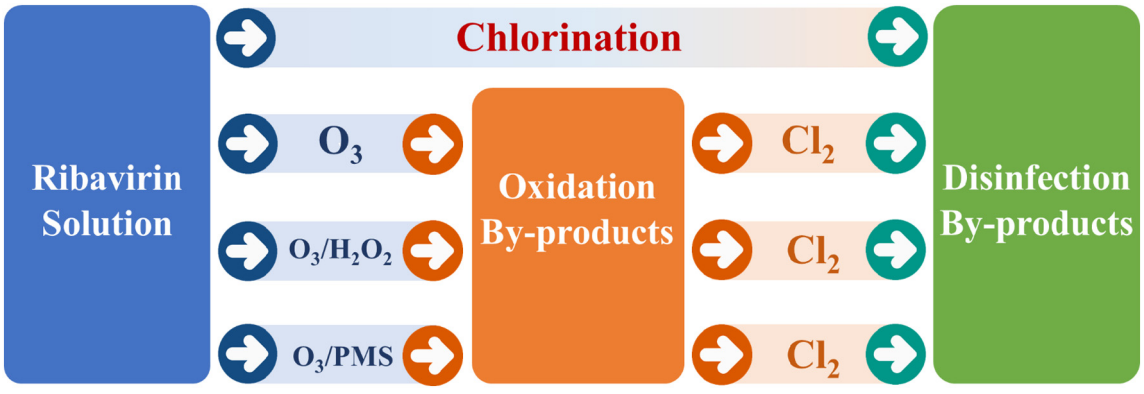

Fig. 1. Schematic diagram of the experimental procedure.

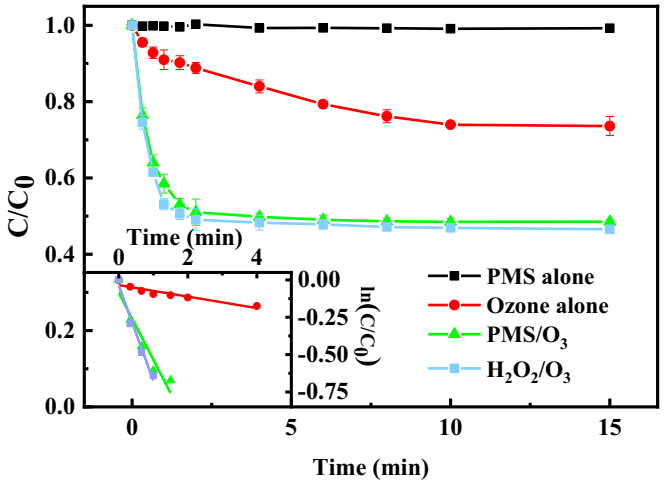

Fig. 2. Degradation of ribavirin by PMS, O_3, O_3/PMS and O_3/H_2O_2. Experiment condition: ribavirin = 10 μM, PMS = 0.025 mM, O_3 = 0.025 mM and pH = 7.0 in 5 mM phosphate buffer.

O_3 accounted for 29.4%, 7.5%, and 11.8% of ribavirin degradation, respectively. The relatively lower contribution of $SO_4^{\bullet-}$ could mainly be attributed to the lower reactivity between ribavirin and $SO_4^{\bullet-}$.

Scavenging experiments employing TBA or MeOH were also performed to investigate the roles of O_3, $SO_4^{\bullet-}$, and •OH in the degradation of ribavirin under different pH and O_3/PMS dosages. MeOH could effectively quench both $SO_4^{\bullet-}$ ($k_{SO4^{\bullet-},\,MeOH} = 1.1 \times 10^7\ M^{-1}\ s^{-1}$) and •OH ($k_{\bullet OH,\,MeOH} = 9.7 \times 10^8\ M^{-1}\ s^{-1}$), while TBA could only effectively quench •OH ($k_{\bullet OH,\,TBA} = 6.0 \times 10^8\ M^{-1}\ s^{-1}$, $k_{SO4^{\bullet-},\,TBA} = 4.0 \times 10^5\ M^{-1}\ s^{-1}$) (Liang and Su, 2009). Thus, the different reactivity of TBA and MeOH toward $SO_4^{\bullet-}$ and •OH can be used to further distinguish the predominant radicals in the O_3/PMS process. The observed first-order degradation rate constant (k_{obs}) of ribavirin under different pH and O_3/PMS dosages with or without scavengers was illustrated in Figs. 4 and S4. •OH played a most important role in the degradation of ribavirin under most conditions, since k_{obs} remarkably decreased when TBA was added. The removal efficiency was largely dependent on pH. With the increase of pH, the k_{obs} increased from $8.1 \times 10^{-2}\ s^{-1}$ to $6.7 \times 10^{-1}\ s^{-1}$. Ribavirin degradation driven by •OH increased significantly from $3.2 \times 10^{-2}\ s^{-1}$ to $3.6 \times 10^{-1}\ s^{-1}$ when pH increased from 6 to 7, then further increased to $5.4 \times 10^{-1}\ s^{-1}$ when pH reached 8. The

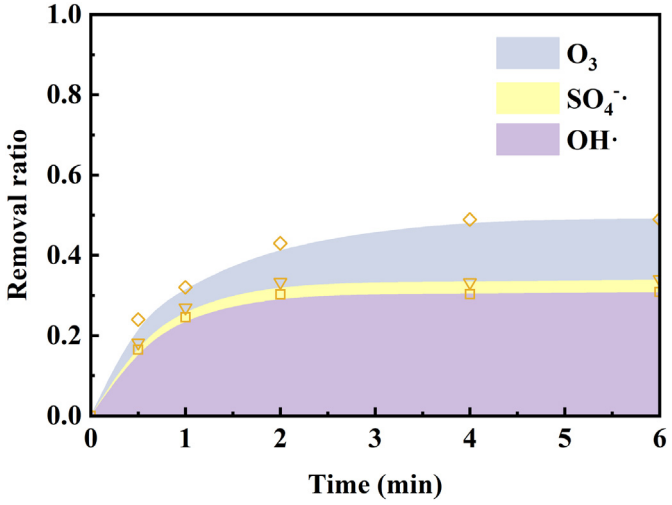

Fig. 3. Contribution of different species to the degradation of ribavirin. Experiment condition: ribavirin = 10 μM, PMS = 0.025 mM, O_3 = 0.025 mM and pH = 7.0 in 5 mM phosphate buffer.

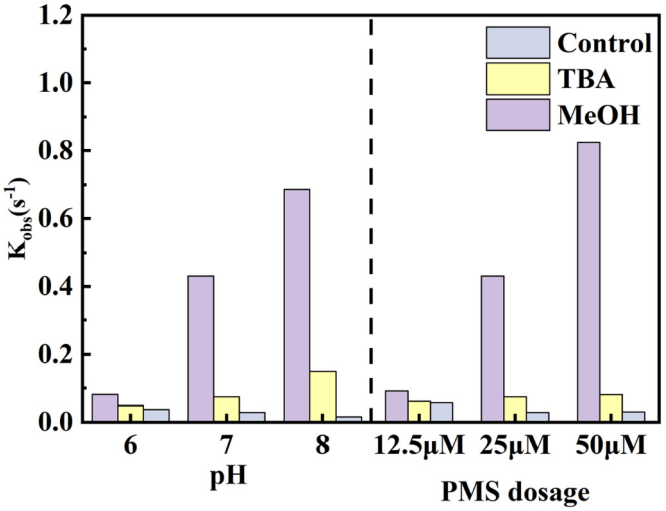

Fig. 4. Inhibition effect of different scavenger on ribavirin degradation with under different pH and different PMS dosage. Experiment condition: ribavirin = 10 μM, PMS = 0.025 mM, O_3 = 0.025 mM, TBA/MeOH = 1 mM and pH = 7.0 with 5 mM phosphate buffer unless specified. None scavenger was added in control group.

ribavirin degraded by $SO_4^{\bullet-}$ also steadily increased with pH, while the contribution of O_3 decreased. These results could be attributed to the follow reasons: 1) the alkaline environment could accelerate the decomposition of O_3 and formation of the reactive •OH (von Gunten, 2003a). Besides, the increased formation of •OH would enhance the formation of $SO_4^{\bullet-}$ through Eqs. (5) and (10) (Mao et al., 2020); 2) pH would affect the speciation of PMS, and the deprotonated PMS (i.e., SO_5^{2-}) was reported to be the main species that reacted with O_3 (Yang et al., 2015). Thus, an alkaline environment, in which PMS generally exists in the deprotonated form, would accelerate the reaction between PMS and O_3 and produce more radicals; 3) at higher pH, $SO_4^{\bullet-}$ would be transformed into •OH (Eq. (9)), and the latter is less selective and reacts rapidly with ribavirin.

$$SO_4^{\bullet-} + OH^- \rightarrow \bullet OH + SO_4^{2-}\ k = 7.3 \times 10^7 M^{-1} s^{-1} \quad (9)$$

$$\bullet OH + SO_5^{2-} \rightarrow OH^- + SO_5^{\bullet-} \quad (10)$$

As the PMS dosage increased from 0.125 mM to 0.5 mM, the k_{obs} increased from $9.1 \times 10^{-2}\ s^{-1}$ to $8.2 \times 10^{-1}\ s^{-1}$. Besides, the contribution of •OH and $SO_4^{\bullet-}$ both increased with the PMS dosage. When the PMS dosage increased form 0.125 mM to 0.5 mM, the contribution of •OH and $SO_4^{\bullet-}$ increased from $3.0 \times 10^{-2}\ s^{-1}$ and $4.6 \times 10^{-3}\ s^{-1}$ to $7.4 \times 10^{-1}\ s^{-1}$ and $5.0 \times 10^{-2}\ s^{-1}$. However, the contribution of O_3 decreased from $5.6 \times 10^{-2}\ s^{-1}$ to $2.9 \times 10^{-2}\ s^{-1}$, then slightly increased to $3.1 \times 10^{-2}\ s^{-1}$. On one hand, increased PMS dosage accelerated O_3 degradation. Previous research showed that the k_{obs} of O_3 consumption increased significantly with PMS when the PMS/ozone ratio was lower than 1:1 (Yang et al., 2015). Therefore, less O_3 was left to react with ribavirin. On the other hand, PMS would compete with ribavirin for O_3 and produce more $SO_4^{\bullet-}$ and •OH, which led to the increased contribution of •OH and $SO_4^{\bullet-}$.

3.3. Effect of water matrix on degradation of ribavirin by O_3/PMS

Inorganics including halide ion and bicarbonate are ubiquitous in water, and could significantly affect the degradation efficiency of AOPs. Therefore, the effect of chloride, bromide, iodide and bicarbonate on the removal of ribavirin by the O_3/PMS process was studied and the results were illustrated in Fig. 5. The existence of low-concentration chloride slightly increases the removal efficiency of the O_3/PMS process. Upon addition of 2 mg/L chloride, the k_{obs} of ribavirin degradation

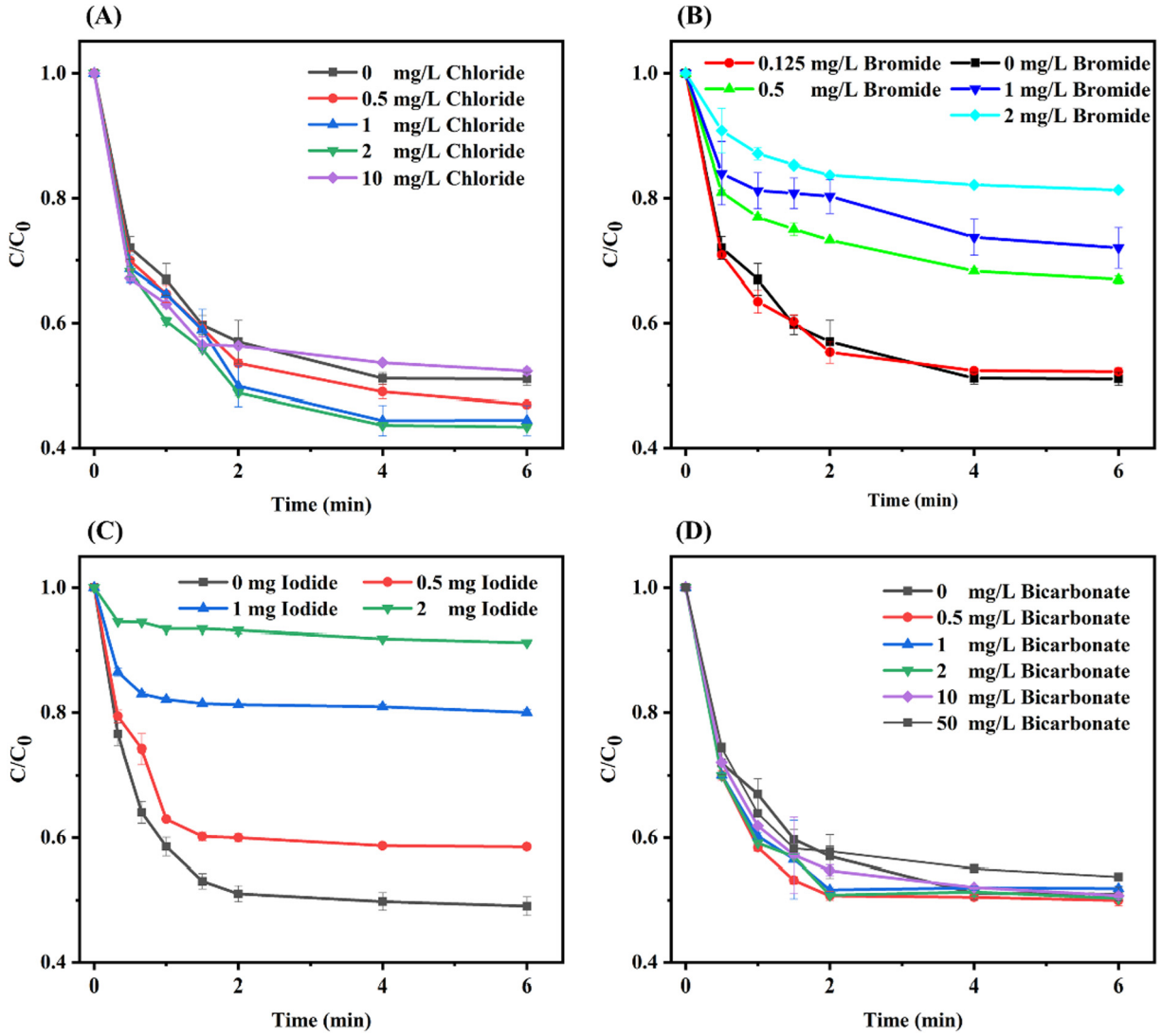

Fig. 5. Effect of chloride (A), bromide (B), iodide (C), or bicarbonate (D) on ribavirin degradation by the activation of ozone with PMS. Experiment condition: ribavirin = 10 μM, PMS = 0.025 mM, O_3 = 0.025 mM and pH = 7.0 with 5 mM phosphate buffer.

increased from 4.32×10^{-1} s^{-1} to 5.05×10^{-1} s^{-1}, and the k_{obs} steadily increased with chloride concentration when the chloride dosage was below 2 mg/L, which was consistent with previous research (Cao et al., 2020). Yang et al. (2014) also observed that the presence of low-level chloride hardly affected the formation of •OH in AOPs. On one hand, the reaction between chloride and •OH is reversible (Eq. (11)), which resulted in limited scavenging effect of chloride on •OH (von Gunten, 2003b). On the other hand, the Cl• formed from the reaction shown in Eq. (13) could be further transformed into •OH via the reverse reactions in Eqs. (11) and (12), and Cl• could rapidly react with ribavirin (Yang et al., 2014). Besides, the Cl• formed from the reaction described in Eq. (12) could also contribute to the degradation of ribavirin (Cao et al., 2020). When the chloride concentration further increased to 10 mg/L, the degradation efficiency of ribavirin decreased to 48%, which can be explained by the consumed Cl• and the formation of less reactive $Cl_2^{\bullet-}$ (Eq. (13)) (Fang et al., 2014; Yang et al., 2014).

Unlike chloride, bromide and iodide would result in lower removal efficiency of ribavirin. As bromide and iodide concentration increased from 0 to 2 mg/L, the k_{obs} of ribavirin degradation decreased from 4.32×10^{-1} s^{-1} to 8.9×10^{-2} s^{-1} and 7.15×10^{-2} s^{-1}, respectively (Fig. 5B and C). Previous research showed that iodide was quickly oxidized to iodate by ozone and PMS, and the half-time HOI/OI^- was extremely short (< 2.0 min and 20 s at pH 7.0 and 8.0, respectively), which could hardly react with DOM during ozonation (Allard et al., 2013; Li et al., 2020). Both of the competition between iodide and ribavirin for oxidation as well as the negligible reactions between the reactive iodine species (RISs) and ribavirin may result in lower removal efficiency. Lu et al. (2020b) found that bromide could enhance the degradation efficiency of ciprofloxacin by O_3 due to the formation of reactive bromine species (RBSs). However, in most cases, bromide would lower the removal efficiency of AOPs (e.g. UV/PS) due to the formation of selective RBSs (Eq. (15)) as a result of the rapid and irreversible reactions between bromide and free radicals (e.g., •OH and SO_4•−) (Wang et al., 2020; Yang et al., 2014). Radicals rather than O_3 played important roles in the elimination of ribavirin during the O_3/PMS process. Thus, similar to iodide, bromide resulted in decreased removal efficiency, and the higher inhibition effect of iodide may be because of the higher reaction rate between iodide and oxidants than bromide, as even PMS alone could rapidly oxidize iodide to iodate (Li et al., 2020).

As Fig. 5D showed, the degradation of ribavirin was hardly affected when the bicarbonate concentration was below 10 mg/L, and the degradation efficiency only slightly decreased when bicarbonate further increased to 50 mg/L. Cao et al. (2020) also observed that bicarbonate significantly suppressed the chloramphenicol degradation only when its concentration exceeded 3.0 mM, and low concentrations of bicarbonate negligibly affected the chloramphenicol degradation during

the O_3/PMS process. The inhibit effect of bicarbonate on micropollutant degradation was commonly observed in AOPs (Cao et al., 2020; Mao et al., 2020). Bicarbonate could transform $SO_4^{\bullet-}$ and •OH into $HCO_3^{\bullet-}$ (Eqs. (17) and (18)). Compared with $SO_4^{\bullet-}$ and •OH, $HCO_3^{\bullet-}$ with lower redox reduction potential of 1.59 V is weak and selective oxidant (Wu and Linden, 2010). Thus, the transformation of $SO_4^{\bullet-}$ and •OH into $HCO_3^{\bullet-}$ led to a decrease in the degradation efficiency.

$$\bullet OH + Cl^- \leftrightarrow ClOH\bullet k = 1.8 \times 10^{10} M^{-1}s^{-1}, k_{reverse} = 6.1 \times 10^9 M^{-1}s^{-1} \quad (11)$$

$$ClOH\bullet + H^+ \leftrightarrow Cl\bullet + H_2O\ k = 7.3 \times 10^5 M^{-1}s^{-1}, k_{reverse} = 2.1 \times 10^{10} M^{-1}s^{-1} \quad (12)$$

$$SO_4^{\bullet-} + Cl^- \rightarrow Cl\bullet + SO_4^{2-}\ k = 3.0 \times 10^8 M^{-1}s^{-1} \quad (13)$$

$$Cl\bullet + Cl^- \leftrightarrow Cl_2^{\bullet-}\ k = 6.5 \times 10^9 M^{-1}s^{-1} \quad (14)$$

$$\bullet OH + Br^- \rightarrow BrOH\bullet\ k = 1.1 \times 10^{10} M^{-1}s^{-1} \quad (15)$$

$$SO_4^{\bullet-} + Br^- \rightarrow Br\bullet + SO_4^{2-}\ k = 3.5 \times 10^9 M^{-1}s^{-1} \quad (16)$$

$$HCO_3^{2-} + \bullet OH \rightarrow HCO_3^{\bullet-} + OH^-\ k = 8.5 \times 10^6 M^{-1}s^{-1} \quad (17)$$

$$HCO_3^{2-} + SO_4^{\bullet-} \rightarrow HCO_3^{\bullet-} + SO_4^{2-}\ k = 9.0 \times 10^6 M^{-1}s^{-1} \quad (18)$$

Humic acid was applied to investigate the effect of DOM on O_3/PMS process, which was illustrated in Fig. 6. As the concentration of humic acid increased to 0.5 mg/L, the k_{obs} of ribavirin degradation slightly decreased from 4.32×10^{-1} s^{-1} to 3.93×10^{-1} s^{-1} and the degradation efficiency further decreased with the humic acid dosage increased. Similar results were also found in the degradation of iopamidol during the O_3/PMS process, which was mainly attributed to the scavenging effect of humic acid (Wu et al., 2019a; Yang et al., 2015). Besides, the fast degradation stage was obviously shortened, which may be related to accelerated O_3 and PMS consumption.

3.4. Proposed transformation pathway

To identify the transformation products of ribavirin during the O_3/PMS process, ESI-tqMS was used to determine the molecular weight of intermediate products. Four transformation products (TPs) were identified, and the product ion spectra of intermediate products were illustrated in Fig. S5. The *m/z* of TP-1 (m/z = 241) was slightly lower than that of ribavirin (m/z = 245), which suggested the increase of unsaturation degree. The multiple losses of 28 (CO) in TP-1 product ion scan spectra revealed that TP-1 may contain at least two carbonyl groups. Besides, the losses of 41 also indicated that the alcoholic group remained intact in TP-1. Therefore, TP-1 may be the product of dehydrogenation on the hydroxyl groups. As for TP-2, the losses of 16 (NH_2) and 28 (CO) suggested that TP-2 may possess amine and carbonyl groups. Considering the m/z of TP-2 (m/z = 211) and TP-1 (m/z = 241), the TP-2 may have originated from TP-1 through loss of alcoholic group. According to the nitrogen rule, there were odd number of nitrogen atoms in TP-3. Besides, the loss of 17 implied that TP-3 may contain hydroxyl group. Thus, TP-3 may be derived from TP-1 via loss of the amide group, and the result of quantum chemical calculation also showed that the amide group may be easily attacked (Table S3). Similar to TP-1, the product ion spectra of TP-4 also illustrated successive losses of 28 (CO). Thus, TP-3 was likely to undergo C—N bond cleavage and hydroxylation and transformed into TP-4. Therefore, a degradation pathway (Fig. 7) was proposed based on the proposed TPs structure.

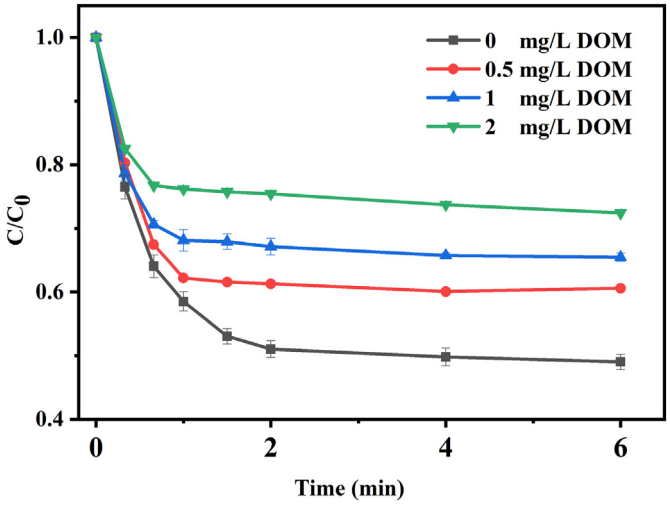

Fig. 6. Effect of DOM on ribavirin degradation. Experiment condition: ribavirin = 10 μM, PMS = 0.025 mM, O_3 = 0.025 mM and pH = 7.0 with 5 mM phosphate buffer.

3.5. OBP formation in the presence of halides during O_3/PMS

Radicals and O_3 could rapidly oxidize halides into reactive halide species, which readily react with DOM and form halogenated OBPs (Wang et al., 2020). Thus, the formation of halogenated OBPs in the presence of different halide ions was evaluated and illustrated in Fig. 8.

$HOBr/OBr^-$ was a crucial intermediate during the oxidation of Br^- by ozonation and the O_3/PMS process, which readily underwent electrophilic reactions and played important roles in the formation of brominated OBPs (von Gunten, 2003b; Wen et al., 2018). Brominated THMs and HALs were the dominant OBPs formed from ozonation and O_3-based AOPs in the presence of bromide, while other OBPs including brominated HNMs and HANs were also detected. The higher yield of carbonaceous OBPs may be attributed to the characteristics of the ribavirin molecule structure. Due to a lack of adjacent carbon atoms, the triazole structure may be hard to form HANs and HNMs (Shah and Mitch, 2012). The concentration of brominated OBPs increased with bromide dosage, which may be associated with increased RBS formation.

Compared to bromide, the formation of chlorinated or iodinated OBPs during the O_3/PMS process in presence of chloride or iodide was negligible. As Table S5 and Fig. S6 showed, most of the chlorinated OBPs were below the limit of detection, and only small amounts of iodoform and monoiodoacetic acid were detected. Similar to brominated OBPs, the formation of iodinated OBPs also increased with iodide concentration. Wu et al. (2019b) also observed that ozonation of chloride-containing wastewater did not increase the total organic chlorine concentration. The low concentration of chlorinated OBPs may be partly attributed to the low reaction rate between chloride and O_3/•OH (von Gunten, 2003b). In contrast, the extremely rapid reactions between RISs (reactive iodide species) and O_3 resulted in short half-lives of RISs, and iodide was completely oxidized to iodate (Allard et al., 2013; Li et al., 2020; von Gunten, 2003b). The increased radical formation during the O_3/PMS process would further shorten the half-lives of RISs. Thus, the formation of iodinated OBPs was limited.

Interestingly, even though chloride could accelerate the degradation of ribavirin, the formation of chlorinated OBPs could be ignored. On the contrary, bromide led to reduced degradation efficiency and the formation of brominated OBPs simultaneously. This phenomenon may be because of different reaction kinetics of bromide and chloride during ozone-based processes. Chloride could hardly be oxidized by O_3. As discussed previously, the accelerated degradation efficiency in presence of chloride was mainly attributed to the increased formation of •OH, which readily occurred oxidation reaction, rather than electrophilic substitution. Therefore, limited chlorinated OBPs were produced. However, the reaction between bromide and oxidants could produce RBSs including $HOBr/BrO^-$ and Br•. Even though the selectivity of RBSs resulted in lower removal efficiency, RBSs readily underwent electrophilic substitution, which resulted in the formation of brominated OBPs.

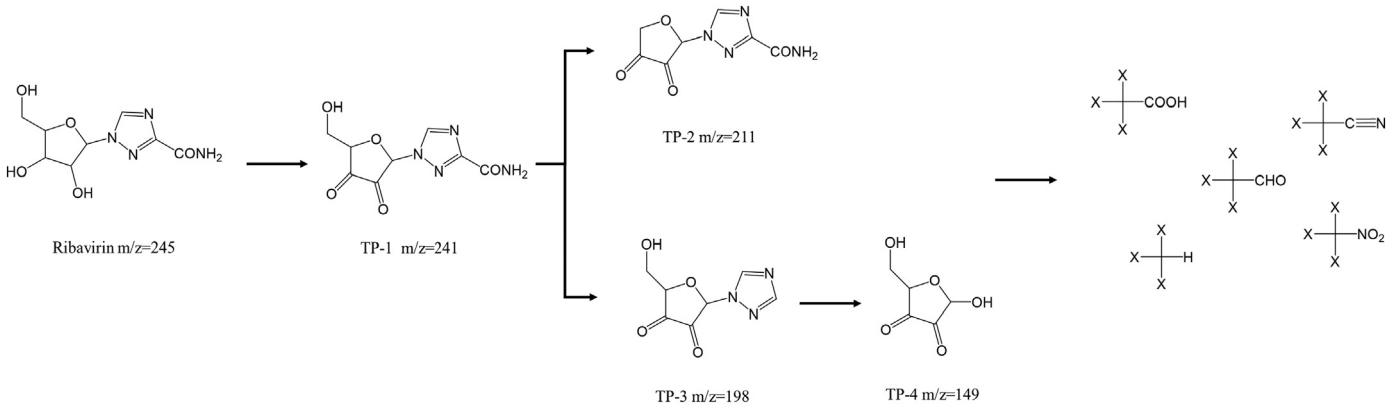

Fig. 7. Proposed degradation pathway of ribavirin during O_3/PMS processes.

As shown in Fig. 8, the formation of OBPs during ozonation and ozone-based AOPs (O_3/PMS, O_3/H_2O_2) in presence of bromide was compared. Similar results for brominated OBP formation were observed during ozonation and the O_3/PMS process, and all of brominated OBPs increased with bromide concentration. The formation of OBPs during ozonation was higher than that during the O_3/PMS process at high bromide concentrations, while the O_3/PMS process produced more brominated OBPs at low bromide concentration. Increased radical induced by PMS could rapidly oxidize HOBr/OBr^- to bromate (Wen et al., 2018). Thus, the concentration of HOBr/OBr^- was decreased, which may reduce the formation of brominated OBPs (Wen et al., 2018; Wu et al., 2020). However, PMS could significantly increase the degradation of ribavirin during ozonation, thus more organic intermediates with lower MW may be produced, which may result in increased brominated OBP formation at high bromide concentration. Besides, at higher bromide concentration, the ozone may outperform O_3/PMS process on ribavirin oxidation, since bromide facilitates ozonation while deteriorates oxidation during O_3/PMS process. Thus, more TPs were available and more OBPs were produced during ozonation than O_3/PMS process at higher bromide.

The formation of brominated OBPs during O_3/H_2O_2 process remained negligible at 2 mg/L bromide. Decreased formation of total organic bromine (TOBr) and brominated OBPs during O_3/H_2O_2 process was also observed in the research by Wu et al. (2020). Previous research showed that adding H_2O_2 could inhibit bromate formation during ozonation because H_2O_2 could readily reduce HOBr/Br^- to bromide, which is crucial to the formation of bromate (Yang et al., 2019). This can also be used to explain the decreased brominated OBP formation when H_2O_2 was added.

Bromate is a commonly recognized DBP of ozonation and ozonation-based processes, and is a potentially carcinogenic compound that has attracted much attention (von Gunten, 2003b; Yang et al., 2019). However, according to Wagner and Plewa (2017), the LC_{50} (the dose of chemical that could show effect in 50% of the population studied) of some brominated OBPs including dibromoacetaldehyde and tribromoacetaldehyde (4.7×10^{-6} M and 3.6×10^{-6} M respectively) were several magnitude lower than that of bromate (9.6×10^{-4} M), which means that the brominated OBPs may possess much higher cytotoxicity than bromate. Wu et al. (2019b) also observed that both the brominated organic matter and bromate contributed to the toxicity of ozonized wastewater. Thus, more attention should be paid to organic OBPs after ozonation and ozone-based processes.

3.6. DBP formation during subsequent chlorination

Ozonation and ozone-based AOP could significantly alter the characteristic of DOM, and further affect the formation of DBPs during subsequent chlorination. Thus, formation of DBPs including THMs, HALs,

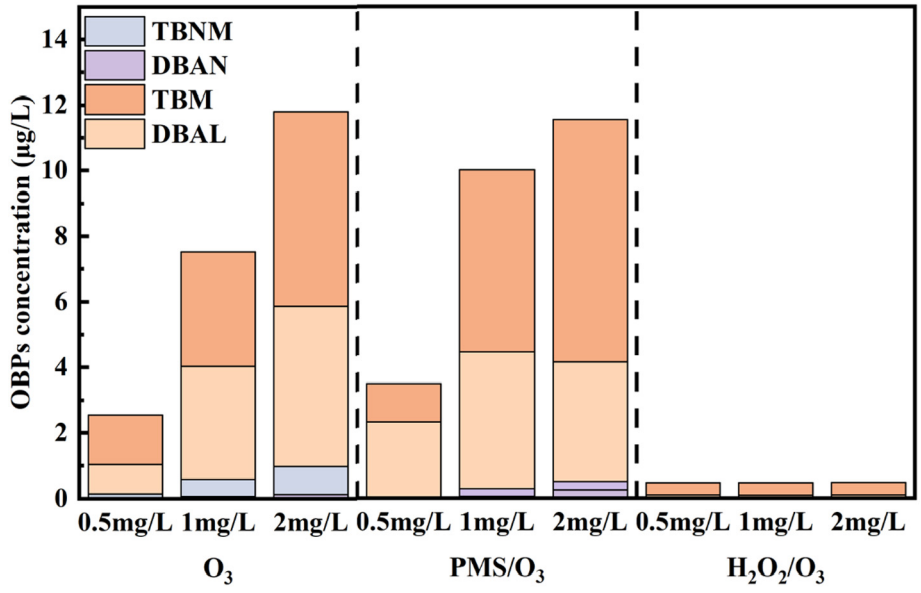

Fig. 8. Formation of OBPs in presence of bromide during ozonation, O_3/PMS and O_3/H_2O_2 process. Experiment condition: ribavirin = 20 μM, PMS/H_2O_2 = 0.025 mM, O_3 = 0.025 mM, pH = 7.0 with 5 mM phosphate buffer.

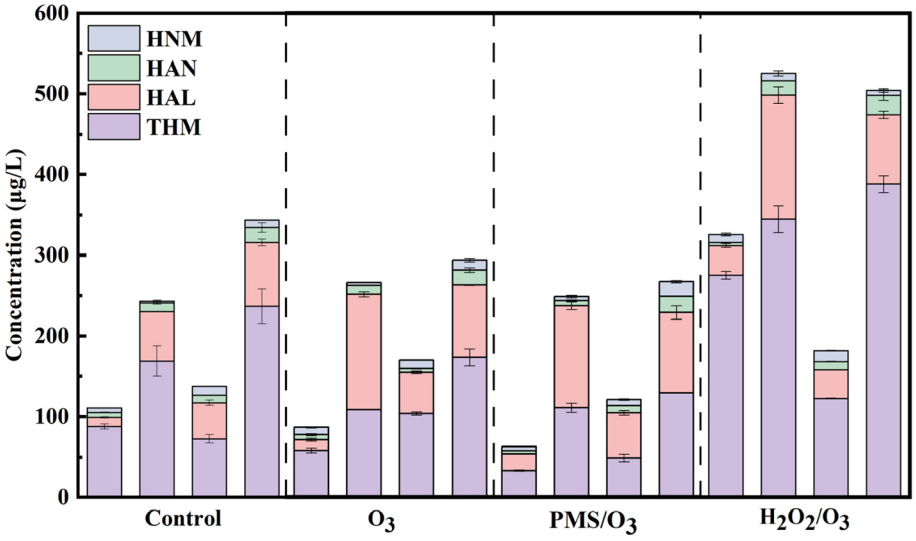

Fig. 9. DBP formation after post chlorination of ribavirin without treatment, with O_3 treatment, with O_3/PMS treatment, and with O_3/H_2O_2 treatment. Experiment condition: ribavirin = 20 μM, PMS/H_2O_2 = 0.025 mM, O_3 = 0.025 mM, pH = 7.0 with 5 mM phosphate buffer. First bar: 4 mg/L chlorine without bromide; Second bar: 4 mg/L chlorine with 0.5 mg/L bromide; Third bar: 8 mg/L chlorine without bromide; forth bar: 8 mg/L chlorine with 0.5 mg/L bromide. None oxidation process was performed before disinfection in control group.

HANs and HNMs during subsequent chlorination was evaluated and illustrated in Fig. 9. The formation of specific DBPs was available in Figs. S7 and S8. The effect of various ozone-based pre-oxidation processes, bromide and chlorine dosages were also investigated.

Similar to OBPs, the concentration of carbonaceous DBPs was much higher than nitrogenous DBPs, and THMs was the first class of DBPs by weight. Compared with control groups, the formation of THMs was slightly decreased after ozonation and the O_3/PMS process. However, after the O_3/H_2O_2 process, the formation of THMs significantly increased by 63.9%–213.0%. This may be attributed to different degradation pathway and different characteristics of TPs. The unselective attack of •OH during O_3/H_2O_2 process may result in hydroxylation or ring-opening reaction of ribavirin, and ribavirin became more reactive to chlorine. Previous research also observed radical •OH-transformed organic matter is more susceptible to halogen incorporation (De Vera et al., 2015). As for HALs, all of the ozonation and ozone-based processes resulted in increased HAL formation, and the promotion effect of the O_3/H_2O_2 process on HAL formation was most obvious (8.0%–213.0%). Similar phenomenon was also observed when ozonation and the O_3/H_2O_2 process were applied to DOM (De Vera et al., 2015; Mao et al., 2018; Yang et al., 2012). Due to negligible decrease in DOC, the slight decrease in THM formation may be attributed to the oxidation of the electronic-rich triazole structure, which led to fewer available halogenation sites for THM formation. As aldehyde and ketone were common oxidation products of ozonation, the increased HALs was reasonable. Considering the relatively lower DBP formation after the O_3/PMS process, PMS may be more suitable than H_2O_2 to enhance the efficiency of ozonation.

Despite being at lower concentration, nitrogenous DBPs have attracted much attention due to their higher cytotoxicity and genotoxicity (Wagner and Plewa, 2017). After ozonation or O_3/PMS process, the formation of HANs was slightly decreased, while the O_3/H_2O_2 process hardly affected the formation of HANs. However, ozonation or ozone-based pre-oxidation resulted in increased formation of HNMs. Those were mainly attribute to oxidation of nitrogenous functional groups including amide and triazole.

The disinfection condition including chlorine dosage could significantly affect the formation and speciation of DBPs. Generally, higher chlorine dosage could result in increased DBP formation, since higher chlorine dosage facilitated chlorination of ribavirin and its TPs. However, the formation of THMs, HANs and HALs was decreased at higher chlorine dosage in some experimental groups. The decreased HALs and HANs may be explained by accelerated hydrolysis induced by excess chlorine.

Bromine is more reactive to DOM than Cl_2 and is prone to forming DBPs than chlorine. Thus, the formation of DBPs in the presence of bromide was much higher than that without bromide (Zhu and Zhang, 2016). With bromide, formation of brominated DBPs was much higher after ozonation and ozone-based processes, and the promotion effect of O_3/H_2O_2 was the most obvious. To better evaluate the effect of ozone and ozone-based processes on DBP speciation, the bromine substitution factor (BSF) of THMs, trihaloacetaldehydes, and trihaloacetonitriles was calculated according to Eq. (19), where m represents the number of bromine and $[CCl_{3-m}Br_mR]$ is the concentration of specific DBPs.

$$BSF = \frac{\sum_{m=1}^{3} m \times [CCl_{3-m}Br_mR]}{3 \times \sum_{m=1}^{3} [CCl_{3-m}Br_mR]} \quad (19)$$

As illustrated in Fig. S9, ozonation and ozone-based process could increase the BSF of THMs by 12%–157%, and the BSF of trihaloacetonitriles was only slightly increased after pre-oxidation. However, the variation of BSF for HALs was not obvious. Similar phenomenon was also observed in previous research where pre-ozonation were applied to natural DOM (Gao et al., 2020; Hua and Reckhow, 2013). Since the concentrations of OBPs formed during pre-oxidation were relatively low, RBSs formed during pre-oxidation may not be the main contributor to the increased brominated DBP formation. Thus, it is more likely that some oxidation products that were more reactive to bromine than chlorine were produced during ozonation and ozone-based processes. However, whether the above phenomenon was similar to that in the presence of DOM needs further investigation.

4. Conclusion

Due to the spread of COVID-19, large amount of antivirals were consumed and released into the environment. This study showed that compared to ozonation, the O_3/PMS process effectively degraded ribavirin via simultaneous •OH and $SO_4^{\bullet-}$ production. As ozonation is commonly used to intensify disinfection during COVID-19, PMS-enhanced ozonation seems to be a convenient and efficiency way to remove antivirals for COVID-19 such as ribavirin from hospital wastewater, part of

which may eventually cycle back to source waters. However, brominated OBPs with high toxicity may be produced during ozonation and the O_3/PMS process in the presence of bromide. Therefore, H_2O_2 rather than PMS is recommended to be used to enhance the ozonation of bromide-containing water. When ozonation is applied as a pre-oxidant with subsequent chlorination, PMS may be more suitable than H_2O_2 to enhance ozonation due to significantly less DBP formation. Further investigations are needed to evaluate the effect of the O_3/PMS process on DBP formation from wastewaters to evaluate the feasibility of its practical application in wastewater treatment, especially for hospital wastewater.

CRediT authorship contribution statement

Xiaoyu Liu: Conceptualization, Data curation, Formal analysis, Investigation, Writing – original draft. **Yuntao Hong:** Investigation, Writing – review & editing. **Shunke Ding:** Formal analysis, Writing – review & editing. **Wei Jin:** Writing – review & editing. **Shengkun Dong:** Writing – review & editing. **Rong Xiao:** Writing – review & editing. **Wenhai Chu:** Conceptualization, Funding acquisition, Project administration, Supervision, Writing – review & editing.

Declaration of competing interest

The authors declare that they have no known competing financial interests or personal relationships that could have appeared to influence the work reported in this paper.

Acknowledgements

This work was funded by National Natural Science Foundation of China (Nos. 52091542, 51822808), International Cooperation Project of Shanghai Science and Technology Commission (No. 20230714100), and Shanghai Soft Science Project (No. 20692113900).

Appendix A. Supplementary material

Supplementary data to this article can be found online at https://doi.org/10.1016/j.scitotenv.2021.148030.

References

Allard, S., Nottle, C.E., Chan, A., Joll, C., von Gunten, U., 2013. Ozonation of iodide-containing waters: selective oxidation of iodide to iodate with simultaneous minimization of bromate and I-THMs. Water Res. 47, 1953–1960.

Cao, Y., Qiu, W., Zhao, Y., Li, J., Jiang, J., Yang, Y., et al., 2020. The degradation of chloramphenicol by O3/PMS and the impact of O3-based AOPs pre-oxidation on dichloroacetamide generation in post-chlorination. Chem. Eng. J. 401, 126146.

Chu, W., Fang, C., Deng, Y., Xu, Z., 2021. Intensified disinfection amid COVID-19 pandemic poses potential risks to water quality and safety. Environ. Sci. Technol. 55, 4084–4086.

Cong, J., Wen, G., Huang, T., Deng, L., Ma, J., 2015. Study on enhanced ozonation degradation of para-chlorobenzoic acid by peroxymonosulfate in aqueous solution. Chem. Eng. J. 264, 399–403.

De Vera, G.A., Stalter, D., Gernjak, W., Weinberg, H.S., Keller, J., Farré, M.J., 2015. Towards reducing DBP formation potential of drinking water by favouring direct ozone over hydroxyl radical reactions during ozonation. Water Res. 87, 49–58.

Fang, J., Fu, Y., Shang, C., 2014. The roles of reactive species in micropollutant degradation in the UV/free chlorine system. Environ. Sci. Technol. 48, 1859–1868.

Fang, C., Ding, S., Gai, S., Xiao, R., Wu, Y., Geng, B., et al., 2019. Effect of oxoanions on oxidant decay, bromate and brominated disinfection by-product formation during chlorination in the presence of copper corrosion products. Water Res. 166, 115087.

Gani, K.M., Hlongwa, N., Abunama, T., Kumari, S., Bux, F., 2021. Emerging contaminants in South African water environment- a critical review of their occurrence, sources and ecotoxicological risks. Chemosphere 269, 128737.

Gao, J., Proulx, F., Rodriguez, M.J., 2020. Effects of ozonation on halogenated acetaldehydes and trihalomethanes formation: strategy of process control for a full-scale plant. J. Water Process Eng. 35, 101205.

Han, J., Zhang, X., 2018. Evaluating the comparative toxicity of DBP mixtures from different disinfection scenarios: a new approach by combining freeze-drying or rotoevaporation with a marine polychaete bioassay. Environ. Sci. Technol. 52, 10552–10561.

Hou, M., Chu, W., Wang, F., Deng, Y., Gao, N., Zhang, D., 2018. The contribution of atmospheric particulate matter to the formation of CX3R-type disinfection by-products in rainwater during chlorination. Water Res. 145, 531–540.

Hua, G., Reckhow, D.A., 2013. Effect of pre-ozonation on the formation and speciation of DBPs. Water Res. 47, 4322–4330.

Hung, I.F.-N., Lung, K.-C., Tso, E.Y.-K., Liu, R., Chung, T.W.-H., Chu, M.-Y., et al., 2020. Triple combination of interferon beta-1b, lopinavir–ritonavir, and ribavirin in the treatment of patients admitted to hospital with COVID-19: an open-label, randomised, phase 2 trial. Lancet 395, 1695–1704.

Lee, J., von Gunten, U., Kim, J.-H., 2020. Persulfate-based advanced oxidation: critical assessment of opportunities and roadblocks. Environ. Sci. Technol. 54, 3064–3081.

Li, J., Jiang, J., Pang, S.Y., Cao, Y., Zhou, Y., Guan, C., 2020. Oxidation of iodide and hypoiodous acid by non-chlorinated water treatment oxidants and formation of iodinated organic compounds: a review. Chem. Eng. J. 386, 123822.

Liang, C., Su, H.-W., 2009. Identification of sulfate and hydroxyl radicals in thermally activated persulfate. Ind. Eng. Chem. Res. 48, 5558–5562.

Liu, X., Chen, L., Yang, M., Tan, C., Chu, W., 2020. The occurrence, characteristics, transformation and control of aromatic disinfection by-products: a review. Water Res. 184, 116076.

Lu, H., Stratton, C.W., Tang, Y.-W., 2020a. Outbreak of pneumonia of unknown etiology in Wuhan, China: the mystery and the miracle. J. Med. Virol. 92, 401–402.

Lu, P., Lin, K., Gan, J., 2020b. Enhanced ozonation of ciprofloxacin in the presence of bromide: kinetics, products, pathways, and toxicity. Water Res. 183, 116105.

Luan, X., Liu, X., Fang, C., Chu, W., Xu, Z., 2020. Ecotoxicological effects of disinfected wastewater effluents: a short review of in vivo toxicity bioassays on aquatic organisms. Environ. Sci. Water Res. Technol. 6, 2275–2286.

M. J. Frisch, G.W.T., Schlegel, H.B., Scuseria, G.E., Robb, M.A., Cheeseman, J.R., Scalmani, G., Barone, V., Petersson, G.A., Nakatsuji, H., Li, X., Caricato, M., Marenich, A.V., Bloino, J., Janesko, B.G., Gomperts, R., Mennucci, B., Hratchian, H.P., Ortiz, J.V., Izmaylov, A.F., Sonnenberg, J.L., Williams-Young, D., Ding, F., Lipparini, F., Egidi, F., Goings, J., Peng, B., Petrone, A., Henderson, T., Ranasinghe, D., Zakrzewski, V.G., Gao, J., Rega, N., Zheng, G., Liang, W., Hada, M., Ehara, M., Toyota, K., Fukuda, R., Hasegawa, J., Ishida, M., Nakajima, T., Honda, Y., Kitao, O., Nakai, H., Vreven, T., Throssell, K., Montgomery Jr., J.A., Peralta, J.E., Ogliaro, F., Bearpark, M.J., Heyd, J.J., Brothers, E.N., Kudin, K.N., Staroverov, V.N., Keith, T.A., Kobayashi, R., Normand, J., Raghavachari, K., Rendell, A.P., Burant, J.C., Iyengar, S.S., Tomasi, J., Cossi, M., Millam, J.M., Klene, M., Adamo, C., Cammi, R., Ochterski, J.W., Martin, R.L., Morokuma, K., Farkas, O., Foresman, J.B., Fox, D.J., 2016. Gaussian 09, Revision A.01.

Malik, S.N., Ghosh, P.C., Vaidya, A.N., Mudliar, S.N., 2020. Hybrid ozonation process for industrial wastewater treatment: principles and applications: a review. J. Water Process Eng. 35, 101193.

Mao, Y., Guo, D., Yao, W., Wang, X., Yang, H., Xie, Y.F., et al., 2018. Effects of conventional ozonation and electro-peroxone pretreatment of surface water on disinfection by-product formation during subsequent chlorination. Water Res. 130, 322–332.

Mao, Y., Dong, H., Liu, S., Zhang, L., Qiang, Z., 2020. Accelerated oxidation of iopamidol by ozone/peroxymonosulfate (O3/PMS) process: kinetics, mechanism, and simultaneous reduction of iodinated disinfection by-product formation potential. Water Res. 173, 115615.

Nannou, C., Ofrydopoulou, A., Evgenidou, E., Heath, D., Heath, E., Lambropoulou, D., 2019. Analytical strategies for the determination of antiviral drugs in the aquatic environment. Trends Environ. Anal. Chem. 24, e00071.

Nannou, C., Ofrydopoulou, A., Evgenidou, E., Heath, D., Heath, E., Lambropoulou, D., 2020. Antiviral drugs in aquatic environment and wastewater treatment plants: a review on occurrence, fate, removal and ecotoxicity. Sci. Total Environ. 699, 134322.

Peng, X., Wang, C., Zhang, K., Wang, Z., Huang, Q., Yu, Y., et al., 2014. Profile and behavior of antiviral drugs in aquatic environments of the Pearl River Delta, China. Sci. Total Environ. 466-467, 755–761.

Peng, L., Wang, F., Zhang, D., Fang, C., van der Hoek, J.P., Chu, W., 2021. Effect of oxidation ditch and anaerobic-anoxic-oxic processes on CX3R-type disinfection by-product formation during wastewater treatment. Sci. Total Environ. 770, 145344.

Postigo, C., Richardson, S.D., 2014. Transformation of pharmaceuticals during oxidation/disinfection processes in drinking water treatment. J. Hazard. Mater. 279, 461–475.

Sellers, R.M., 1980. Spectrophotometric determination of hydrogen peroxide using potassium titanium(IV) oxalate. Analyst 105, 950–954.

Shah, A.D., Mitch, W.A., 2012. Halonitroalkanes, halonitriles, haloamides, and N-nitrosamines: a critical review of nitrogenous disinfection byproduct formation pathways. Environ. Sci. Technol. 46, 119–131.

Tan, C., Cui, X., Sun, K., Xiang, H., Du, E., Deng, L., et al., 2020. Kinetic mechanism of ozone activated peroxymonosulfate system for enhanced removal of anti-inflammatory drugs. Sci. Total Environ. 733, 139250.

von Gunten, U., 2003a. Ozonation of drinking water: part I. Oxidation kinetics and product formation. Water Res. 37, 1443–1467.

von Gunten, U., 2003b. Ozonation of drinking water: part II. Disinfection and by-product formation in presence of bromide, iodide or chlorine. Water Res. 37, 1469–1487.

Wagner, E.D., Plewa, M.J., 2017. CHO cell cytotoxicity and genotoxicity analyses of disinfection by-products: an updated review. J. Environ. Sci. 58, 64–76.

Wang, Z., An, N., Shao, Y., Gao, N., Du, E., Xu, B., 2020. Experimental and simulation investigations of UV/persulfate treatment in presence of bromide: effects on degradation kinetics, formation of brominated disinfection byproducts and bromate. Sep. Purif. Technol. 242, 116767.

Wen, G., Qiang, C., Feng, Y., Huang, T., Ma, J., 2018. Bromate formation during the oxidation of bromide-containing water by ozone/peroxymonosulfate process: influencing factors and mechanisms. Chem. Eng. J. 352, 316–324.

Wong, C.K.H., Wan, E.Y.F., Luo, S., Ding, Y., Lau, E.H.Y., Ling, P., et al., 2021. Clinical outcomes of different therapeutic options for COVID-19 in two Chinese case cohorts: A propensity-score analysis. EClinicalMedicine 32, 100743.

Wu, C., Linden, K.G., 2010. Phototransformation of selected organophosphorus pesticides: roles of hydroxyl and carbonate radicals. Water Res. 44, 3585–3594.

Wu, G., Qin, W., Sun, L., Yuan, X., Xia, D., 2019a. Role of peroxymonosulfate on enhancing ozonation for micropollutant degradation: performance evaluation, mechanism insight and kinetics study. Chem. Eng. J. 360, 115–123.

Wu, Q.-Y., Zhou, Y.-T., Li, W., Zhang, X., Du, Y., Hu, H.-Y., 2019b. Underestimated risk from ozonation of wastewater containing bromide: both organic byproducts and bromate contributed to the toxicity increase. Water Res. 162, 43–52.

Wu, Q.-Y., Yang, L.-L., Zhang, X.-Y., Wang, W.-L., Lu, Y., Du, Y., et al., 2020. Ammonia-mediated bromate inhibition during ozonation promotes the toxicity due to organic byproduct transformation. Environ. Sci. Technol. 54, 8926–8937.

Yang, X., Peng, J., Chen, B., Guo, W., Liang, Y., Liu, W., et al., 2012. Effects of ozone and ozone/peroxide pretreatments on disinfection byproduct formation during subsequent chlorination and chloramination. J. Hazard. Mater. 239-240, 348–354.

Yang, Y., Pignatello, J.J., Ma, J., Mitch, W.A., 2014. Comparison of halide impacts on the efficiency of contaminant degradation by sulfate and hydroxyl radical-based advanced oxidation processes (AOPs). Environ. Sci. Technol. 48, 2344–2351.

Yang, Y., Jiang, J., Lu, X., Ma, J., Liu, Y., 2015. Production of sulfate radical and hydroxyl radical by reaction of ozone with peroxymonosulfate: a novel advanced oxidation process. Environ. Sci. Technol. 49, 7330–7339.

Yang, J., Dong, Z., Jiang, C., Wang, C., Liu, H., 2019. An overview of bromate formation in chemical oxidation processes: occurrence, mechanism, influencing factors, risk assessment, and control strategies. Chemosphere 237, 124521.

Ye, D., Bao, Z., Yu, Y., Han, Z., Yu, Y., Xu, Z., et al., 2020. Inhibition of cardiomyocyte differentiation of human induced pluripotent stem cells by ribavirin: implication for its cardiac developmental toxicity. Toxicology 435, 152422.

Zhu, X., Zhang, X., 2016. Modeling the formation of TOCl, TOBr and TOI during chlor(am)ination of drinking water. Water Res. 96, 166–176.